Earth Interactions • Volume 20 (2016) • Paper No. 3 • Page 1

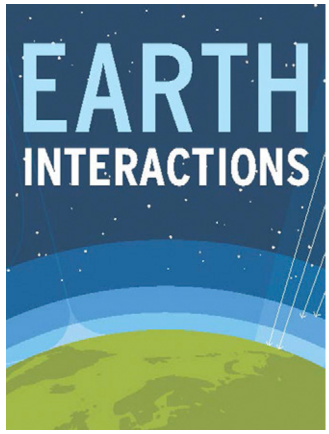

The Effects of Weather and Environmental Factors on West Nile Virus Mosquito Abundance in Greater Toronto Area

E.-H. Yoo*

University at Buffalo, Buffalo, New York

D. Chen

Department of Geography, Queen's University, Kingston, Ontario, Canada

Chunyuan Diao

University at Buffalo, Buffalo, New York

Curtis Russell

Enteric, Zoonotic and Vector-Borne Diseases, Public Health Ontario, Toronto, Ontario, Canada

Received 19 December 2014; in final form 13 October 2015

---

* Corresponding author address: E.-H. Yoo, Department of Geography, University at Buffalo, Buffalo, NY 14261.

E-mail address: eunhye@buffalo.edu

DOI: 10.1175/EI-D-15-0003.1

ABSTRACT: We investigated how weather conditions and environmental factors affect the spatiotemporal variability in *Culex pipiens* population using the data collected from a surveillance program in Ontario, Canada, from 2005 to 2008. This study assessed the relative influences of temperature and precipitation on the temporal patterns of mosquito abundance using harmonic analysis and examined the associations with major landscape predictors, including land-use type, population density, and elevation, on the spatial patterns of mosquito abundance. The intensity of trapping efforts on the mosquito abundance at each trap site was examined by comparing the spatial distribution of mosquito abundance in relation to the spatial intensity of trapping efforts. The authors used a mixed effects modeling approach to account for potential dependent structure in mosquito surveillance data due to repeated observations at single trap sites and/or similar mosquito abundance at nearby trap sites each week. The model fit was improved by taking into account the nested structure of mosquito surveillance data and incorporating the temporal correlation in random effects.

KEYWORDS: Mathematical and statistical techniques; Spectral analysis/models/distribution; Models and modeling; Model comparison; Applications; Disease; Geographic information systems (GIS); Land use

1. Introduction

Global warming and wide fluctuation in weather contributed to the emergence of West Nile virus (WNV) data across most of the United States of America by 2002 and further spread to Canada and Central America by 2004 (Epstein 2005; Hayes et al. 2005; Komar and Clark 2006; DeGroote et al. 2014). As warmer summers and shorter winters are more frequently encountered, blood feeding and reproductive activity are accelerated (Soverow et al. 2009). It is important to understand how weather affects WNV in order to inform control efforts. Many studies have shown that the abundance of city-dwelling and bird-biting *Culex pipiens* mosquitoes is strongly linked to the transmission of WNV (Epstein 2005; Bolling et al. 2009; Kilpatrick and Pape 2013) and have suggested that identifying habitat associations and spatiotemporal distributions of the vector species is a key to implement effective control strategies (Diuk-Wasser et al. 2006; Rosà et al. 2014).

Developing a robust spatiotemporal model that predicts mosquito population dynamics is a challenging task because mosquito abundance is determined by complex interactions among weather, land-use, and vegetation coverage as well as the blood meal availability and intensity of mosquito control efforts. Our understanding of the effects of weather and environmental factors is limited, and the availability of data at a fine spatial and temporal resolution is not guaranteed. Data contaminated by measurement error may further hamper our efforts to improve the understanding of mosquito feeding behavior and population dynamics. While it has not drawn enough attention, ignoring the dependence structure underlying mosquito surveillance data may lead to underestimation of standard errors in linear regression models and invalid conclusions (Jones 2004; Zuur et al. 2009; Yoo et al. 2014).

In the current paper, we aimed to identify predictors of spatiotemporal variation in the *Culex pipiens* population in Ontario, Canada, with the ultimate goal of facilitating the monitoring efforts of WNV transmission risk. To achieve the goal, we assessed the relative influence of temperature and precipitation on the temporal patterns of mosquito abundance using harmonic analysis, which is a promising tool to characterize time series data in the frequency domain by effectively eliminating noise in the original data (Moody and Johnson 2001). We also examined the relative influence of major landscape predictors, including land-use type, population density, and elevation, on the spatial patterns of mosquito abundance. Last, we used a mixed effects modeling approach to account for the nested structure of the data due to the surveillance design and the presence of potential dependent structures in random effects. To demonstrate the potential pitfalls by ignoring or misspecifying the random effects and their structure in the surveillance-based WNV mosquito abundance model, we proposed four statistical models and provided model comparison results.

2. Background

Culex pipiens mosquitoes lay their eggs in water and require aquatic habitats for their larva development (Horsfall 1955; Merritt et al. 1992). Rainfall is important in creating and maintaining suitable larval habitats, but excess rainfall would flush the drains and catch basins and thus strongly affects the abundance of adult mosquitoes (Epstein 2001). Meanwhile, high temperatures increase the abundance of mosquitoes and accelerate the development of WNV within the mosquitoes (Epstein 2001; Dohm et al. 2002; Reisen et al. 2006; Soverow et al. 2009; Wang et al. 2011). Local environmental conditions also increase the potential for mosquito breeding. In urban structures, for example, stagnant rivers and streams are prevalent and artificial containers of water are numerous along with high numbers of catch basins, and these provide habitats for *Culex pipiens* (Deichmeister and Telang 2011). Vegetation density also contributed to mosquito abundance as trees and shrubs may offer resting habitats to adult mosquitoes and roosting for birds (Chuang et al. 2011; Gardner et al. 2013).

Given that climatic constraints have significant effects on the transmission of WNV, many researchers have examined and documented the factors associated with WNV transmissions over the United States (Anderson et al. 2006; Gingrich et al. 2006; Ruiz et al. 2010; Chuang et al. 2012). However, the spatial distribution and the study of landscape influences on WNV transmission and mosquito abundance are still under investigation. Based on a recent literature review, we summarized influential weather conditions and environmental factors associated with *Culex pipiens* in Table 1.

3. Data

3.1. Mosquito surveillance data

The greater Toronto area (GTA) is the largest urban agglomeration in Canada. The study area consists of four health regions—Hamilton, Peel, city of Toronto, and York—with a population size of 3 328 590 (2006 census) and diverse land uses. Mosquito data were obtained from a surveillance program conducted by the Ontario Ministry of Health and Long-Term Care, which collects adult female mosquitoes on a weekly basis. More specifically, the Ontario mosquito surveillance system used U.S. Centers for Disease Control (CDC) light traps that attract host-seeking mosquitoes via both CO_2 and ultraviolet light. During the mosquito season, traps were placed at the beginning of the week for one night and were collected the following morning and then submitted to a service provider who would sort, identify, and test certain species. The total of 7812 records were collected over 4

Table 1. Literature review on the effects of weather and environmental conditions on *Culex pipiens*. CDD^{base} is the cooling degree days with base temperature (base) $= 0.5(T_{max} + T_{min}) - T_{base}$; DD^{base} is the degree weeks with base temperature $= \begin{cases} T_{mean} - T_{base} & \text{if } T_{mean} \geq T_{base} \\ 0 & \text{otherwise} \end{cases}$; T_l is the temperature at the lth lagged week (°C); P_l is the precipitation at the lth lagged week (mm); $\overline{T}_{a-b}$ is the average temperature between weeks a and b; $\overline{P}_{a-b}$ is the average precipitation between weeks a and b disease water stress index $\frac{\text{near infrared} + \text{Green}}{\text{short infrared} + \text{Red}}$; and AMSR-E: NASA Advanced Microwave Scanning Radiometer for Earth Observing System (EOS).

	Variables	Source	Study Area	Reference
Weather Conditions	$CDD^{17.2°C}$	Weather station	Western New York	Trawinski and MacKay (2008)
	$DW^{22°C}$	Weather stations	Illinois	Ruiz et al. (2010)
	$DW^{9°C}$, P_5	Weather station	Ontario, California	Wang et al. (2011)
	T_0, T_1, P_3, P_4	Weather stations	South Dakota	Chuang et al. (2011)
	T_0, T_1, P_1, P_2, P_3	Weather stations	South Dakota	Chuang et al. (2012)
	T_0, T_1, water fraction	AMSR-E		
	T_0, T_1, P_1, daytime length, relative humidity, wind speed	Weather station	Illinois (41°9′N)	Lebl et al. (2013)
	T	MODIS	Northwestern Italy (45°0′N)	Rosà et al. (2014)
Environmental Factors	NDVI	Landsat	Queens, New York	Brownstein et al. (2002)
	NDVI, disease water stress index, distance to the nearest waterbody	ASTER	New Haven, Connecticut	Brown et al. (2008)
	NDVI, land use, population density, housing unit density, age of dwellings	USGS	Erie County, New York	Trawinski and MacKay (2010)
	Proximity to drainage	The Henrico County Public Works Department	Henrico County, Virginia	Deichmeister and Telang (2011)
	Tree density, areas of shrubs of height $\leq$ 1 m	Onsite survey	Chicago, Illinois	Gardner et al. (2013)
	NDVI, elevation, slope, land use	County spatial database	Shelby County, Tennessee	Ozdenerol et al. (2013)

years between 2005 and 2008 from 341 trap sites. In the study region, the mosquito season lasts about 17 weeks between late May and October (weeks 24–40).

3.2. Weather and environmental factors

Daily temperature and precipitation data were obtained from the Toronto weather station (Toronto Pearson, Ontario). To match the temporal scale of mosquito data, weekly weather variables, including average temperature and accumulated precipitation, were computed and used in the analysis. Following Kilpatrick et al. (2008), we considered 14°C the minimum temperature threshold for amplification of WNV in *Culex pipiens* in the study area and calculated the fraction of the number of weeks below the threshold temperature during the trap season ($F_{\mathrm{MinT} \leq 14C^{\circ}}$) each year (see Table 3). Based on the weekly average temperature, we created a variable of degree week (DW) with a base temperature of 14°C (Reisen et al. 2006; Ruiz et al. 2010).

The land-use data of GTA have seven classes—waterbody, residential, commercial, government and industry, open area, parks/recreational, and resources—which were aggregated into four major classes: water surface, built-up area (residential, commercial, government, and industry), open area, and vegetation area (parks/recreational and resources). To analyze the association between land use and *Culex pipiens*, we calculated the proportion of reclassified land-use type within 1-km-radius buffer zones centered at mosquito trap sites. The size of buffer zone was less than the maximum flight distance of *Culex pipiens* (Ciota et al. 2012; Diuk-Wasser et al. 2006). We also included both elevation and normalized difference vegetation index (NDVI) as environmental predictors, which were available at the spatial resolution of 250 m. Last, population data at the census tract level in 2006 were used to create a dummy variable for urban and rural area. If a trap site was located in a census tract whose population was above 1000 and a population density over 400 persons per square kilometer, the value for the urban variable was 1, and it was 0 otherwise. Covariates used in the study and their sources are summarized in Table 2.

4. Statistical methodology

For an exploratory data analysis, we used harmonic analysis and kernel density estimation as a means of characterizing temporal and spatial patterns of mosquito abundance. Both methods have been widely used to explore the majority of the temporal and spatial variations because of their insensitivity to the inherent noise in the data. The harmonic analysis is particularly efficient to capture a long-term trend and short-term variations of data through the first few harmonic components, whereas the kernel density method effectively describes the spatial intensity of mosquito surveillance data than other sophisticated methods (O'Sullivan and Unwin 2003). We further developed spatiotemporal mosquito abundance models using a mixed effect modeling framework to explicitly account for site-specific or week-specific differentials in mosquito abundance.

4.1. Harmonic analysis

Harmonic analysis (also known as Fourier analysis) decomposes time series data, such as the average number of *Culex pipiens* per trap night and temperature, in the

Table 2. Description of covariates and data sources.

Variables	Data	Source
Weekly average temperature	Daily weather conditions	National Climate Data and Information Archive, Environment Canada
Weekly accumulated precipitation		
Built-up area	Land use*	Land Information Ontario
Water surface		
Vegetation area		
Open area		
Elevation	Canadian digital elevation data	GeoBase
NDVI	Moderate Resolution Imaging Spectroradiometer (MODIS) 16-day vegetation index products	NASA
Urban indicator	2006 census	Stats Canada

* Proportion of reclassified land-use type within a buffer of radius 1 km centered at each trap site.

frequency domain to capture their seasonal changes and intra-annual trends (Legates and Willmott 1990; Justino et al. 2011). As a result, the complex time-dependent periodic phenomenon is characterized with an additive term and a series of sine and cosine waves (Briggs and Henson 1995; Jakubauskas et al. 2001; Moody and Johnson 2001). The additive term is the arithmetic mean value over the time series, where each decomposed wave is defined by a unique amplitude and phase value. The phase represents the offset between the origin and the peak of the wave, whereas amplitude denotes half the height of the wave. Successive harmonic terms are added to simulate the original time series curve. That is, the variance of a time series is equal to the sum of the variances of all harmonic terms and the percent of variance for each decomposed wave is calculated by dividing the individual variance by the total variance (Jakubauskas et al. 2001; Davis 2002). Similar to principal component analysis, the majority of the variance can often be explained by the first few components. The equation of harmonic analysis can be written as

$$f(x) = c_0 + \sum_{n=1}^{\infty} c_n \cos\left(\frac{2\pi n}{N}x - \phi_n\right), \tag{1}$$

where c_0 is the arithmetic mean value of a time series, and c_n and ϕ_n are the amplitude and phase angle of the nth-order trigonometric, respectively. The length of the time series is denoted by N, that is, 52 corresponding to the weekly sampling rate in our study. Each order designates a decomposed wave with a unique cycle. When n equals one, c_1 and ϕ_1 are the amplitude and phase value of the first-order trigonometric, and the decomposed wave is unimodal with only one cycle over the time series. For example, the mean value of the harmonic of temperature denotes the average temperature over the year, while the amplitude and the phase value of the first-order harmonic indicates the variation and seasonal range of the temperature and the time of the maximum temperature, respectively. Further details about harmonic analysis can be found in Jakubauskas et al. (2001) and Moody and Johnson (2001).

4.2. Kernel density estimation

Kernel density estimation (KDE) is used to summarize spatial density of trapping efforts and mosquito abundance. The spatial density of trap sites can be calculated by placing the surface at each trap location and evaluating the distance between the trap site and a reference point using a mathematical (kernel) function. The kernel density value at that reference location is obtained by summing the value for all the surfaces (Silverman 1986; Anderson 2009). The resulting surface is typically smooth and continuous, although the level of smoothness is controlled by the choice of the kernel bandwidth. Bandwidths that are too large are likely to produce an overly smooth surface where density estimates are similar everywhere, but those that are too small are likely to produce a surface that focuses only on individual trap sites. As suggested by O'Sullivan and Unwin (2003), we have chosen the bandwidth for KDE of mosquito trapping efforts and mosquito abundance as the half of its maximum flying range of *Culex pipiens*, that is, 1 km (U.S. Environmental Protection Agency 2004).

4.3. Statistical model development

We examined associations of weather and environmental conditions with spatiotemporal distributions of *Culex pipiens* using the mean pooled mosquito abundance per trap and per night, respectively. The effects of weather conditions on the mean pooled mosquito abundance per trap night were assessed under the consideration of weather variables up to five prior weeks. Correlations with the harmonic predictions of weekly average temperature and precipitation were also calculated. Influential landscape variables were also identified by correlation analyses between the site-specific mean abundance and multiple landscape variables, including the areal proportion of the major land-use type around trap locations, NDVI, elevation, and the indicator variable for an urban/rural area. Based on the correlation analyses and guided by a stepwise linear regression, we selected influential weather and environmental variables for a spatiotemporal WNV mosquito abundance model, which can be written as

$$Y_{ij} = \beta_{0ij} + \beta_1 \mathbf{X}_{1j} + \beta_2 \mathbf{X}_{2i}, \tag{2}$$

where Y_{ij} denotes the square root transformed mosquito data observed at the ith trap site with coordinates $\mathbf{s}_i = (x_i, y_i)$, $i = 1, \ldots, 341$ and at the jth trap night with t_j, $j = 1, \ldots, 68$. The time-indexed variables, including an indicator for the year of observation and harmonic predictions of temperature and 5 weeks of accumulated precipitation, are denoted as $\mathbf{X}_{1j}$, and three landscape predictors, which consist of the proportion of vegetation areas within the 1-km buffer zones, elevation, and the proportion of built-up area in the urban setting, are denoted as $\mathbf{X}_{2i}$.

As shown in the previous studies (Yoo 2013, 2014; Yoo et al. 2014), the variability in the mosquito abundance per trap and per night could be substantial. Thus, mixed effects models are an efficient and effective means to account for site-specific or trap night–specific differentials in mosquito abundance. We extended the "fixed effects model" in Equation (2), referred to as model A, to mixed effects models that shared the same covariates with model A but differed in terms of their random effect specification and error structures.

Table 3. Descriptive statistics for weekly *Culex pipiens* and weather conditions during 2005 and 2008. $F_{\mathrm{MinT}\le 14^\circ\mathrm{C}}$ is the fraction of weeks with minimum temperature is below 14°C during trap weeks (weeks 24–40).

	Mosquito counts				Sites	Trap nights	Weather conditions		
Year	Total	Max	Mean	Std dev	Total	Total	Mean temperature	Mean precipitation	$F_{\mathrm{MinT}\le 14C^\circ}$
2005	12 141	231	6.15	14.82	224	1818	20.06	2.69	0.24
2006	14 523	418	7.73	22.86	140	1879	20.06	2.69	0.18
2007	7470	113	3.82	10.10	141	1958	18.75	3.76	0.41
2008	23 331	210	11.54	22.84	145	2022	19.37	2.88	0.18

In the fixed effects model, the intercept β_{0ij} was defined as a sum of an overall mean mosquito abundance β_0 and purely random errors ε_{ij}. On the other hand, random effects models (models B and C) take explicit account for the nested structure of the dependent variable: multiple observations taken per trap night and at each trap site, respectively. Models B and C do not assume any systematic structure for their random effects, whereas model D in Equation (5) assumes that the random effects for each trap site have a temporal correlation. The random effects of models B, C, and D are summarized below as the combination of the overall mosquito abundance β_0 across sites and trap nights, random effects for a trap night u_i, random effects for a trap v_j, and within-group errors ε_{ij}:

$$\beta_{0ij} = \beta_0 + u_i + \varepsilon_{ij}, \quad u_i \sim N(0, \sigma_u^2), \quad \varepsilon_{ij} \sim N(0, \sigma_\varepsilon^2), \tag{3}$$

$$\beta_{0ij} = \beta_0 + v_j + \varepsilon_{ij}, \quad v_j \sim N(0, \sigma_v^2), \quad \varepsilon_{ij} \sim N(0, \sigma_\varepsilon^2), \tag{4}$$

$$\beta_{0ij} = \beta_0 + v_j + \varepsilon_{ij}, \quad v_j \sim N[0, \sigma_v^2(\mathbf{h})], \quad \varepsilon_{ij} \sim N(0, \sigma_\varepsilon^2). \tag{5}$$

We further assumed that the covariance structure of random effects is a function of the lag distance $\mathbf{h}$ between any pair of trap nights, which takes a form of an exponential function $\sigma_v^2(\mathbf{h}) = b\exp(-\mathbf{h}/r)$. The nugget effects and range parameters, denoted as b and r, were estimated from observed data. The unit of the range parameter r for model D is weeks.

5. Results

5.1. Spatiotemporal distribution of *Culex pipiens* abundance

Total of 23 331 adult females per trap night in 2008 tripled the previous year's record (7470 counts) despite similar trap nights—1958 records in 2007 and 2022 records in 2008. As summarized in Table 3, trap nights for the 4 years were comparable, although there was a change in trapping strategy over the years. That is, the number of trapping frequency at each trap site increased over the 4 years but the total number of sites employed decreased since 2006. The highest record of females per trap night was on week 27 of 2006 (a total of 418), and the second highest was on week 33 of 2008 (210).

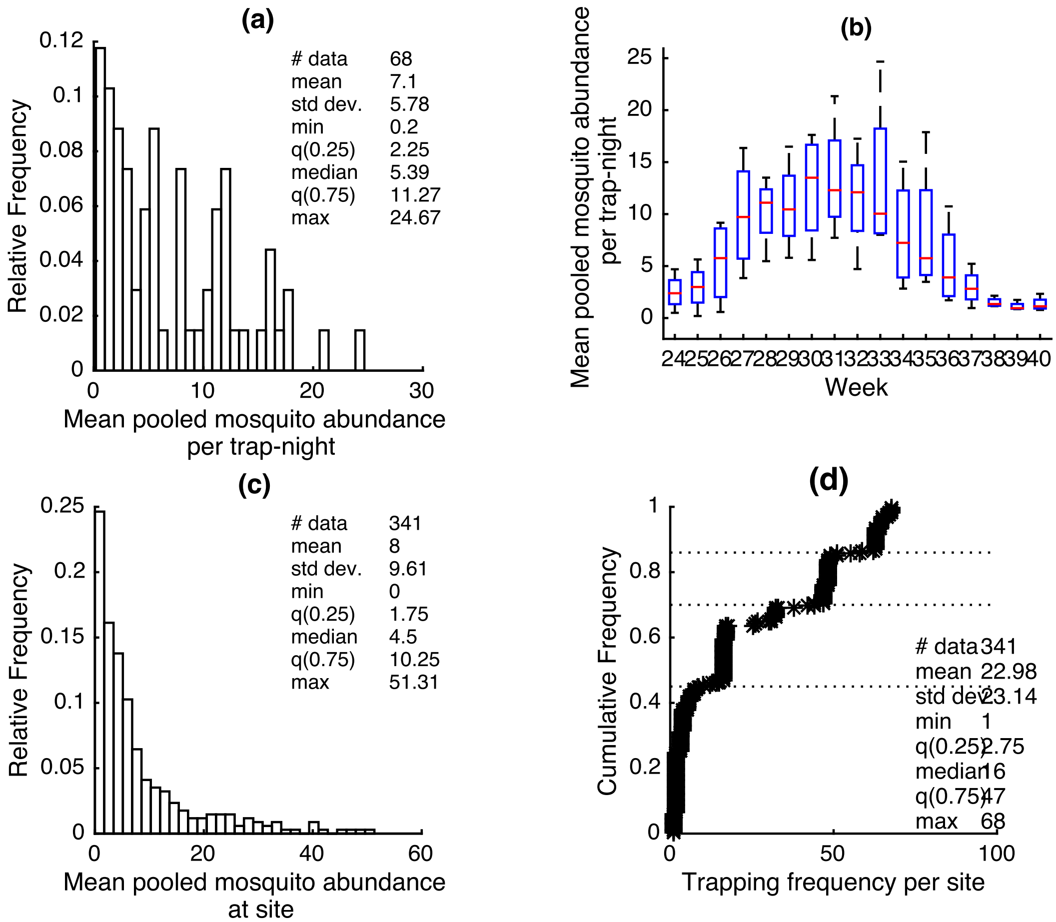

Figure 1. Spatiotemporal pattern of mosquito abundance data: (a) spatial average of female mosquitoes per trap night, (b) spatial averages of female mosquitoes per trap night by week, (c) temporal average of female mosquitoes per trap site, and (d) the number of trap nights per site.

To characterize the temporal distribution of female mosquito abundance, we calculated the mean pooled mosquito abundance per trap night. The mean pooled abundance of *Culex pipiens* per trap night ranges between 0.20 and 24.67 with an average of 7.10. Large zero values are also shown in Figure 1a, and the weekly variation in mosquito abundance is well summarized by the box plot in Figure 1b. Over the 4 years, mosquito abundance during week 29–33 was higher than the average abundance (7.10) with yearly variation: a total of 11 weeks were above the 4-yr average in 2008, but only 3 weeks later in the season (week 31 to 33) were above the average in 2007. We also noticed that the high mosquito abundance season lasted longer in 2008 (up to week 36), whereas the typical peak season ended at week 33 in the other 3 years.

It is necessary to understand the effects of different trapping efforts per site in quantifying site-specific mosquito abundance. Only 6 trap sites out of a total of 341 sites were consistently operated during the 4 years of the study period. The average

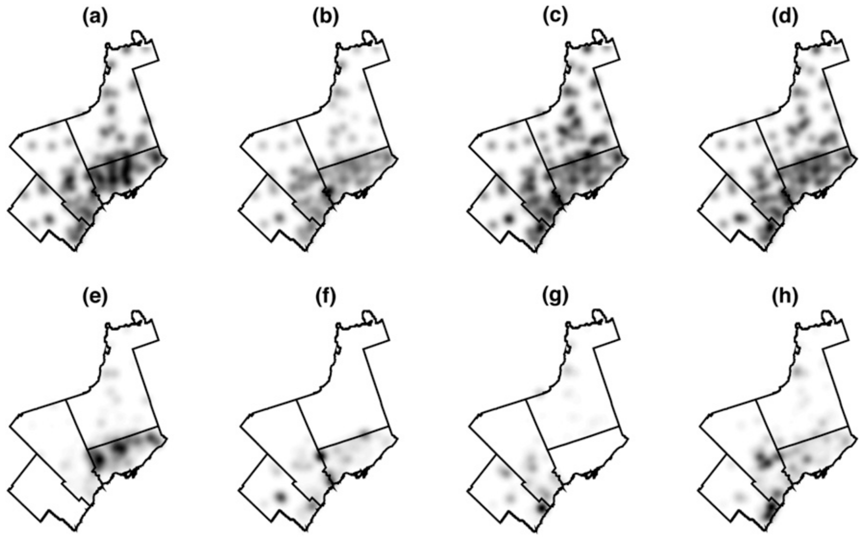

Figure 2. Kernel density estimation of the number of trap weeks and mosquito population in the year of (a),(e) 2005; (b),(f) 2006; (c),(g) 2007; and (d),(h) 2008.

number of trap nights at each site was 23 with a standard deviation of 23.14 over 4 years. As shown in the empirical cumulated density function of trapping frequency per site in Figure 1d, half of the sites had less than 16 trap nights and 75% of sites had 47 trap nights. Similar to the mean pooled mosquito abundance per trap night summarized in Figure 1a, we calculated the mean pooled mosquito abundance at each site by dividing the total number of *Culex pipiens* captured at each trap site by the total number of trap nights. The mean pooled mosquito abundance may be quite different from the total number of mosquitoes captured at each site due to the differences in trap nights at each site. The mean pooled mosquito abundance at each trap site form a positively skewed distribution that ranges between 0 and 51.31 with an average of 8.00 and a standard deviation of 9.61 [see Figure 1c].

The spatial density of trap sites operated each year was calculated using KDE, and the results are shown in Figures 2a–d. A total of 224 trap sites were operated in 2005, mostly concentrated in the city of Toronto [Figure 2a], but in 2006 half of the trap sites were closed. In both years of 2007 and 2008, the spatial distribution of trap sites was rather evenly distributed across the study area. Meanwhile mosquito abundance per year has been shifted from the city of Toronto in 2005 to the region of Hamilton and Peel from 2006 to 2008. Particularly, there was substantial increase in mosquito abundance along the coastal area of the Lake Ontario since 2006. The spatial distribution of mosquito abundance per year is presented in Figures 2e–h. Mosquito intensity has increased in Hamilton since 2006 and expanded into a larger area without substantial changes in trap sites. The visual inspection of two maps in Figures 2c and 2g suggested that the mosquito abundance of the city of Toronto in 2007 was lower than any other region in the study area despite the intense trapping efforts made. The association of trapping efforts with mosquito abundance at each trap site was further examined by calculating correlation between the total number of observation weeks

Table 4. Amplitude and phase values for the first harmonics of the discrete Fourier transform for the time series variables.

		2005	2006	2007	2008
Mosquito abundance	Mean	5.53	8.08	4.11	11.58
	Amplitude I	5.86	6.52	3.30	9.85
	Phase I	30.77	29.95	30.23	31.35
Temperature	Mean	10.57	10.56	8.34	9.18
	Amplitude I	11.66	11.66	13.26	12.75
	Phase I	29.32	29.46	29.61	30.16
Precipitation	Mean	12.60	12.61	13.37	11.49
	Amplitude I	2.33	2.39	5.20	4.16
	Phase I	37.91	37.28	29.85	27.90

and the trap site–specific average mosquito counts per year. We found little to no associations between them as suggested by the low correlation coefficients for 2005 to 2008 as -0.06, -0.05, -0.15, and 0.03, respectively.

5.2. Harmonic analysis

We performed a harmonic analysis to characterize the seasonal pattern of mean pooled mosquito abundance per trap night and weather variables such as weekly average temperature and 5-week precipitation accumulation. Harmonic predictions of the three temporal variables were calculated each year, and the results are summarized in Table 4 and Figure 3. The variability in the mosquito abundance and average temperature was mostly captured by the first harmonic, which had a much larger amplitude value than the successive components. The mean of the first harmonic for mosquito abundance and average temperature each year in Table 4 matched with their yearly variability summarized in Table 3.

The summary statistics of original weather variables in Table 3 indicated that the annual average temperature of 2007 and 2008 was slightly lower than that of 2005 and 2006, whereas the fraction of weeks with minimum temperature below 14°C was smallest in 2008 (0.18) and largest in 2007 (0.41). Harmonic analysis captured this yearly variability as well as the seasonality when the peak of temperature occurred; the peak occurred at week 29 in the first 3 years, as shown in the phase I values of 2005 to 2007, but hot summer lasted longer in 2008, as evidenced in the larger phase I value 30. We selected only the first three harmonics to simulate the original time series because most variability was explained for both variables.

Unlike the first two variables, it was challenging to capture the intrinsic trend of precipitation by the harmonic analysis, and thus we incorporated more harmonic terms to explain the temporal variability in precipitation. Unusually large precipitation in 2007 (447 mm) was summarized by the harmonic mean 13.37 mm. The seasonality summarized by phase I values was substantially different in accumulated precipitation, as that of 2008 was earlier in week 28 than other years. Figure 3 illustrated the harmonic predictions of the three variables each year.

5.3. Correlation analysis and model development

For a correlation analysis with weather conditions, we considered the following five variables—weekly average temperature, accumulated precipitation,

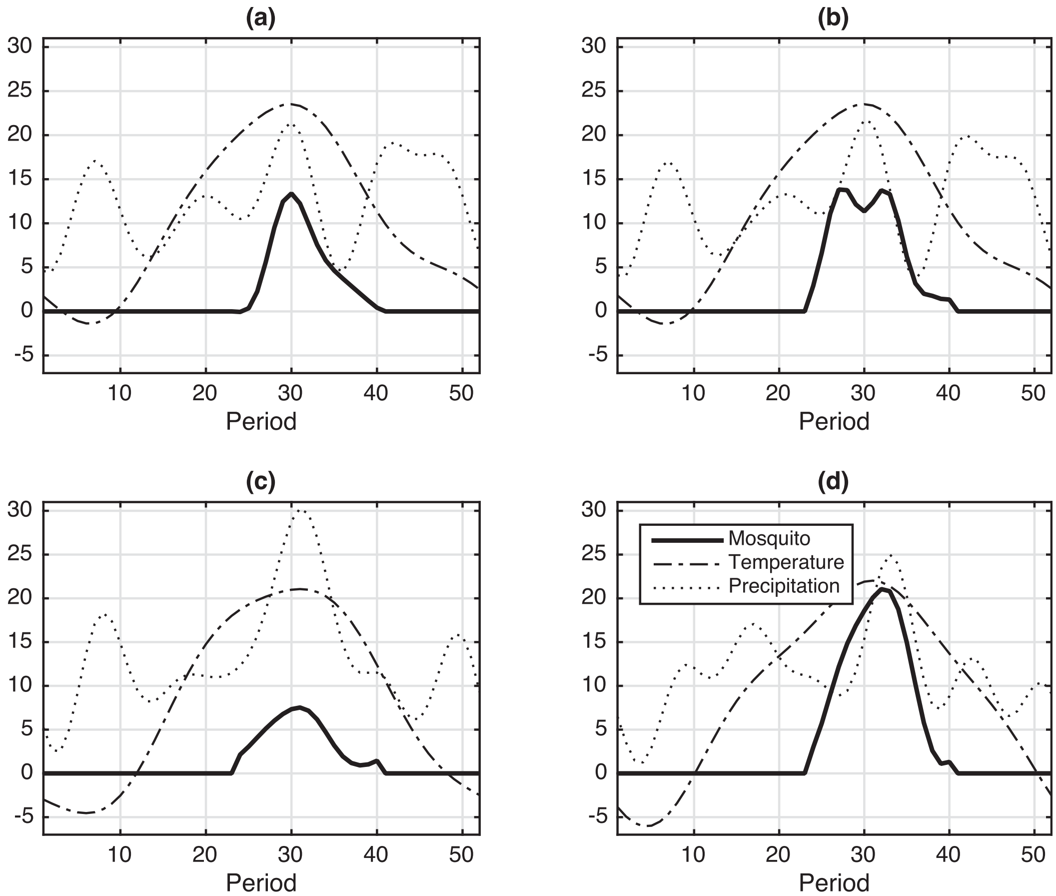

Figure 3. Harmonic predictions of weekly mosquito abundance, weekly average temperature, and accumulated precipitation (5 weeks prior to observation) in the year of (a) 2005, (b) 2006, (c) 2007, and (d) 2008.

degree weeks based on 14°C ($DW^{14°C}$), and the harmonic predictions of temperature and accumulated precipitation—across multiple lags. The results summarized in Table 5 clearly show the delay effects of weather conditions, particularly precipitation, on the mosquito population abundance. The temperature-derived variables—average temperature, DW, and the harmonic predictions of average temperature—showed relatively strong correlation with mosquito abundance, while the harmonic predictions of temperature were the strongest at 0.71. The correlation of mosquito abundance with precipitation variables was comparable at 0.43 for the harmonic predictions of accumulated precipitation and 0.41 for the original variable.

We also examined the associations of trap site–specific mean pooled mosquito abundance with environmental factors around the trap sites, such as elevation, NDVI, population density, and the proportion of land use within the spatial buffer centered at each trap site. We found that mosquito abundance was negatively correlated with the elevation of the trap site (−0.24) and the proportion of open space within 1-km buffer around trap sites (−0.20) but positively correlated with the proportion of vegetation areas (0.19) and urban area (0.15). The correlation

Table 5. Correlation analysis with weather variables at multiple lags.

	Lag 0	Lag 1	Lag 2	Lag 3	Lag 4	Lag 5
Average temperature	0.61[a]	0.59[a]	0.56[a]	0.40[a]	0.26[b]	0.17
Accumulated $DW^{14°C}$	0.62[a]	0.66[a]	0.67[a]	0.68[a]	0.64[a]	0.59[a]
Average precipitation	0.08	0.25[b]	0.32[c]	0.38[c]	0.40[a]	0.41[a]
Harmonic temperature	0.69[a]	0.71[a]	0.65[a]	0.49[a]	0.28[b]	0.11
Harmonic precipitation	0.42[a]	0.43[a]	0.33[c]	0.15	−0.09	−0.33[c]

[a] $p < 0.001$.
[b] $p < 0.05$.
[c] $p < 0.01$.

with NDVI and the proportion of open waterbody surrounding trap sites was weak and negative as −0.08 and −0.07, respectively.

Based on the exploratory analysis of spatially and temporally marginal mosquito abundance, we selected the variables with the most influential effects on the spatial and temporal variability in mosquito abundance per trap per night. Some variables, such as average temperature, NDVI, and proportion of open space in affinity of trap sites, were correlated with the mosquito abundance, but they were not included in the final model because of their collinearity with other variables. The covariates of the spatiotemporal WNV mosquito prediction model in Equation (2) included an indicator variable for the year of observation, two weather variables (harmonic predictions of average temperature of coincident week and accumulated precipitation up to prior 5 weeks), and three environmental variables (elevation, the proportion of vegetation areas within the 1-km buffer zone, and the proportion of built-up area in urban setting).

5.4. Model fit and validation

Table 6 summarizes the four WNV mosquito abundance models fit by restricted maximum likelihood (REML). The two weather variables and three landscape predictors were statistically significant across all four models. The yearly variation in mosquito abundance was reflected in the sign of model coefficient estimates: increased mosquito abundance in the year of 2006 and 2008 matched with the positive coefficient estimates for the corresponding dummy variables. Model coefficient estimates of the fixed effects model (model A) confirmed the results of correlation analysis showing that the temperature of the same week of mosquito data collection and accumulated precipitation are important predictors of mosquito abundance. The negative association of mosquito abundance with the elevation (−0.08) of trap sites was also statistically significant. The two land-use types surrounding trap sites include vegetation areas, such as parks and forest, and built-up areas in the urban setting.

We assessed the residuals of the model A in terms of its normality and temporal and spatial correlation structure. Figure 4a shows the distribution of residuals overlaid with normal density with the same mean and variance. The long tail in high values and the absence of low values of the residuals may violate a strict normality assumption, but the sample size (7677) is large enough to alleviate the problem. Figures 4b and 4c show the variogram and autocorrelation (ACF) plot of

Table 6. Results of statistical model estimates. I(.) denotes the indicator (dummy) variable, and P(.) denotes the proportion of the land-use type.

	Model A	Model B	Model C	Model D
Fixed effects				
(Intercept)	−0.18(0.02)[a]	−0.19(0.04)[a]	−0.14(0.04)[a]	−0.22(0.04)[a]
I(2006)	0.13(0.03)[a]	0.14(0.04)[a]	0.18(0.03)[a]	0.20(0.05)[a]
I(2007)	−0.07(0.03)[b]	−0.09(0.03)[c]	−0.07(0.03)[b]	−0.03(0.05)
I(2008)	0.37(0.04)[a]	0.41(0.05)[a]	0.32(0.04)[a]	0.41(0.06)[a]
Harmonic temperature	0.26(0.01)[a]	0.23(0.02)[a]	0.25(0.01)[a]	0.28(0.01)[a]
Harmonic precipitation	0.19(0.01)[a]	0.14(0.02)[a]	0.20(0.01)[a]	0.18(0.01)[a]
Elevation	−0.08(0.01)[a]	−0.08(0.01)[a]	−0.09(0.04)[c]	−0.07(0.03)[b]
P(Green)	0.12(0.01)[a]	0.12(0.01)[a]	0.14(0.04)[a]	0.11(0.03)[a]
P(Built up) × I(Urban)	0.08(0.02)[a]	0.08(0.02)[a]	0.11(0.05)[b]	0.09(‘0.04)[b]
Random effects				
Level 2		$\hat{\sigma}_u^{2}$[d]	$\hat{\sigma}_v^{2}$[e]	$\hat{\sigma}_\varepsilon^{2}$[f]
	NaN	0.19^2	0.43^2	0.18^2
Level 1				
$\hat{\sigma}_\varepsilon^2$	0.91^2	0.90^2	0.83^2	0.84^2
$(\hat{b}, \hat{r})$				(0.45, 6.76)
AIC	20 761.17	20 668.39	19 742.54	17 021.34
Bayesian Information Criterion (BIC)	20 830.79	20 744.98	19 819.13	17 111.62
Log likelihood	−10 370.59	−10 323.20	−9860.27	−8497.67

[a] $p < 0.001$.
[b] $p < 0.05$.
[c] $p < 0.01$.
[d] Trap week effects.
[e] Trap site effects.
[f] Trap site effects with temporal correlation.

the residuals, respectively, which indicate the presence of temporal autocorrelation but not strong spatial dependence in residuals.

The two unstructured random effects models (models B and C) improved models fit as shown in the smaller Akaike information criterion (AIC). Compared with the AIC of fixed effects model, the AIC decreased (20 668.39) when the differentials of mosquito abundance for trap nights in model B were taken into account and further decreased (19 742.54) when the random effects for trap sites were considered in model C. When the two random effects models (models B and C) were compared using a likelihood ratio test, however, the improvement of model C with the smaller AIC than model B was not statistically significant.

We also examined the correlation structure of the two random effects models: for the spatial autocorrelation in random effects at each week in model B and the temporal autocorrelation of random effects at each trap site in model C. The empirical variograms of random effects were calculated for both models, and the results are shown in Figures 4d and 4e. Figure 4d did not reveal any systematic pattern in random effects of model B, whereas Figure 4e clearly indicated the presence of temporal autocorrelation of model C.

For modeling the temporal autocorrelation structure for the random effects in model D, we considered both an autoregressive model of order 6 and an exponential correlation function in Equation (5). Both correlation structure models improved the model fit based on AIC values—17 051.75 for the AR(6) model and

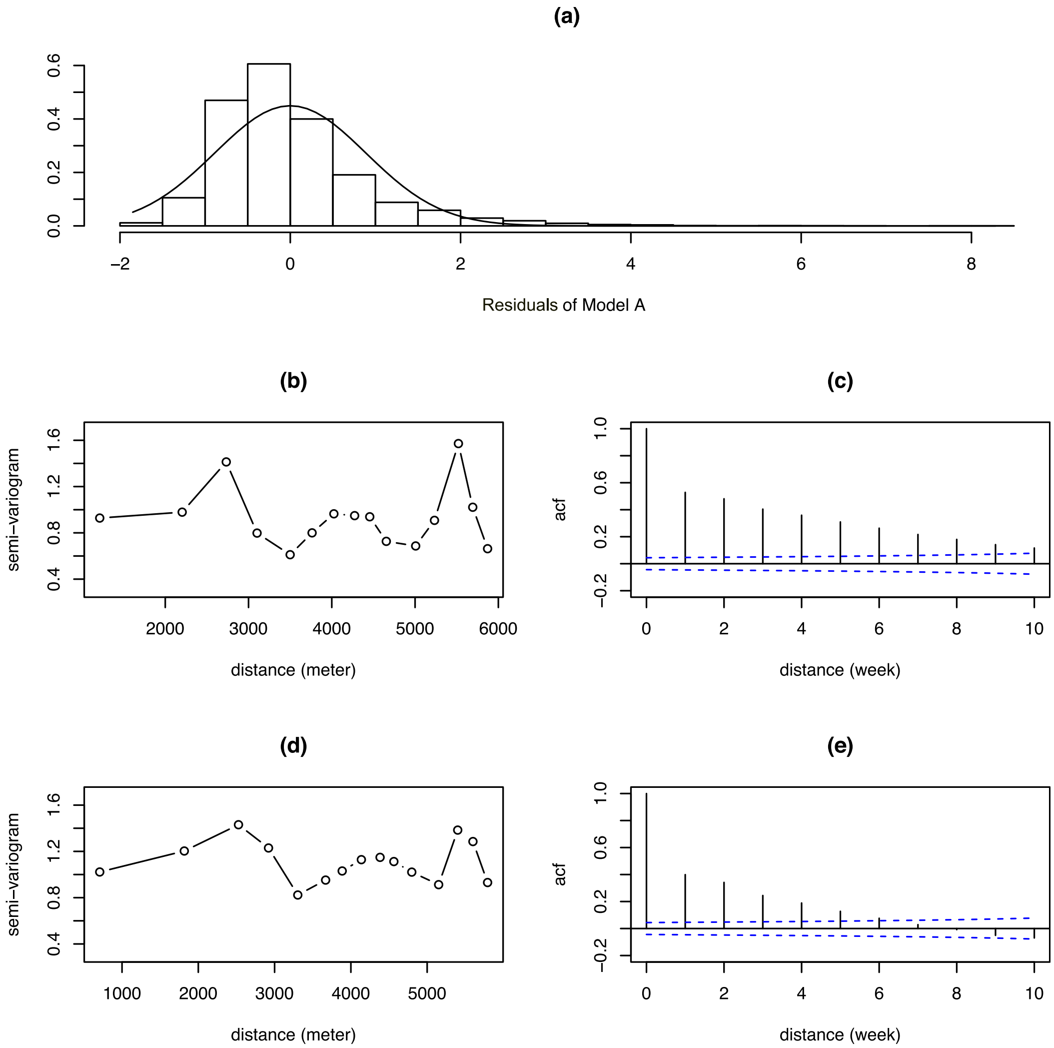

Figure 4. (a),(b),(c) Histogram, variogram, and autocorrelation function (ACF) of Model A residuals, respectively. (d) The variogram of random effects of Model B. (e) The ACF of random effects of Model C.

17 021.34 for the exponential model, which were lower than those of other three models, but we imposed an exponential correlation function for the temporal correlation structure for the random effects in model D due to the model parsimony. The parameters for range and nugget effects were estimated as 6.70 and 0.45, respectively (see Table 6). The random effects models did not have a direct impact on the fixed effects estimates except for model B where the explicit consideration of trap nights affected both weather variables—harmonic prediction of temperature dropped to 0.23 from 0.26 and precipitation to 0.14 from 0.19. However, random effects models affected the quality of the fixed effects through the standard errors of the slopes for the fixed effects—standard errors of all predictors in model D are

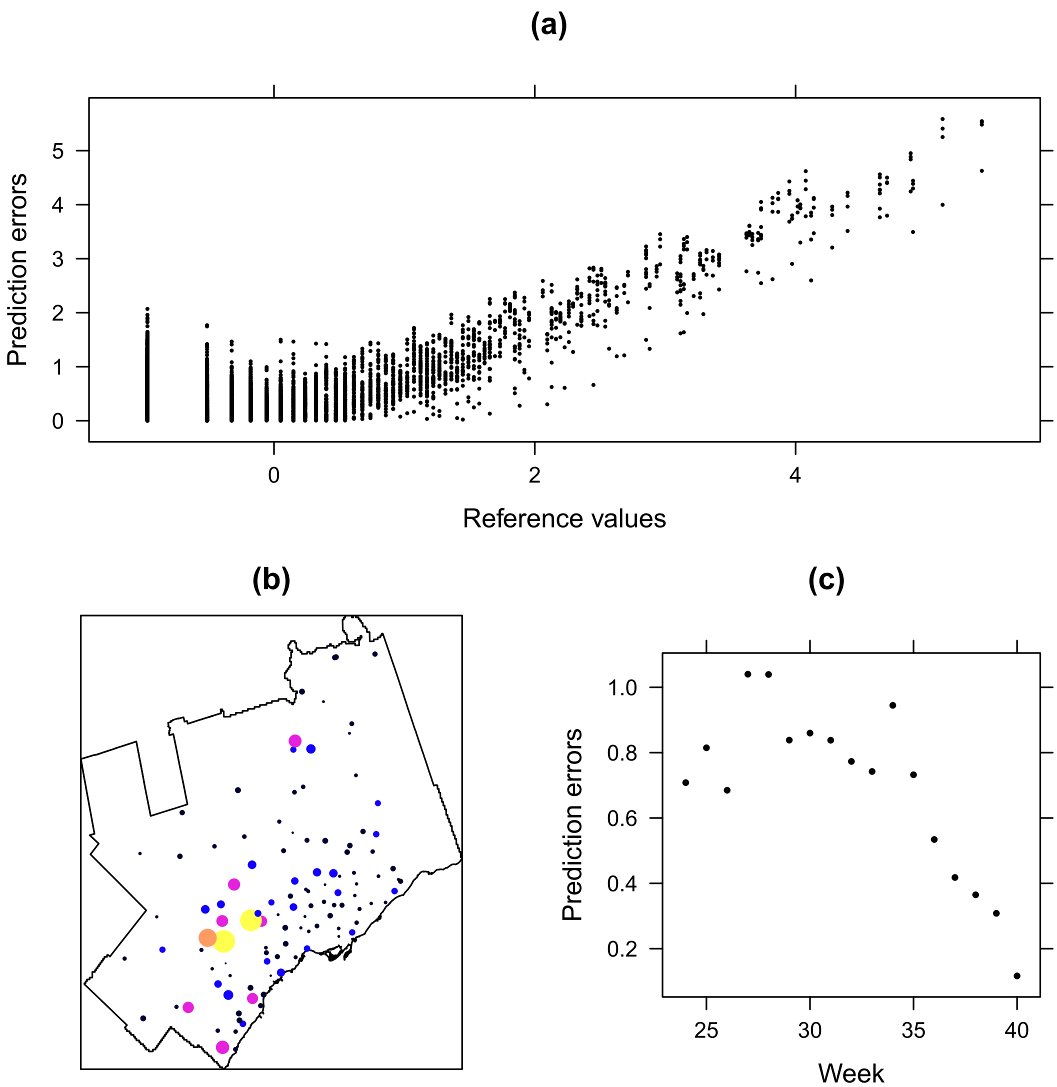

Figure 5. Distribution of model prediction errors; (a) pooled model prediction errors vs reference values, (b) spatial average of prediction errors per trap site, and (c) temporal average of prediction errors per trap night. The large circles with bright colors (yellow, orange, and magenta in order) in the regions of Peel and Hamilton indicate that large prediction errors and the high mosquito abundance per trap nights in 2009 were concentrated in these regions. The smaller circles with dark colors (black and blue) represent the smaller prediction errors

greater than or equal to those of model A. In addition, the within-group error estimates $\hat{\sigma}_{\varepsilon}^{2}$ decreased in model D as the variation in mosquito abundance not modeled in terms of fixed effects was incorporated in mixed effects models.

Last, we evaluated model prediction performance with mosquito surveillance data collected from 110 sites between week 24 and 40 in 2009. We used all four models to predict female mosquito abundance at 1597 trap nights. The predicted mosquito

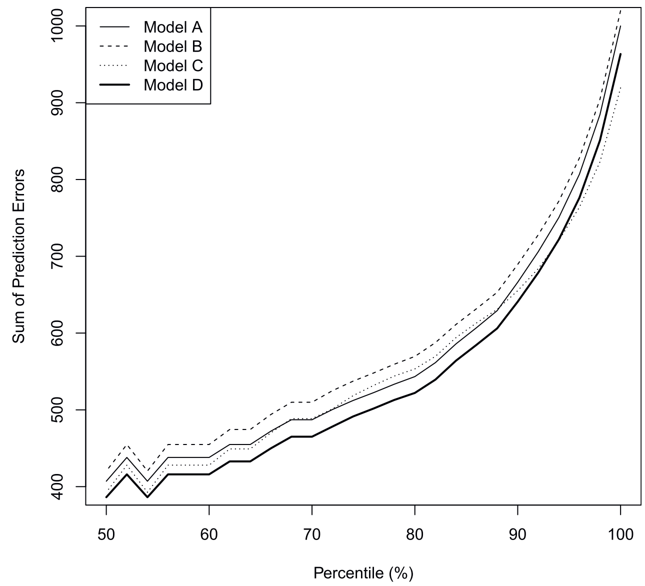

Figure 6. Sensitivity of model predictability to extreme values.

abundance was compared with the observation and the sum of absolute values of prediction errors, that is, the difference between the predicted abundance and the observed mosquito abundance was calculated. Prediction errors were larger for the higher values of validation data across all four models. The results are illustrated in Figure 5a, where the pooled model prediction errors matched for corresponding reference values. The spatial and temporal patterns of prediction errors are also illustrated in Figures 5b and 5c, respectively. The circle symbols in Figure 5b represent the magnitude of prediction errors at the locations of 110 trap sites. The large circles in the regions of Peel and Hamilton indicate that large prediction errors and the high mosquito abundance per trap nights in 2009 were concentrated in these regions. The temporal distribution of prediction errors also indicates pooled mean mosquito abundance per trap night in 2009, where unusually high abundance was observed at the weeks of 27, 28, and 34. We further conducted a sensitivity analysis of model validation by taking a subset of validation data. The four model prediction performance was evaluated using the 50th to 100th percentile of 2009 mosquito abundance data. The result is summarized in Figure 6 where the sum of prediction errors of the four models is plotted over the percentile of data used. The prediction accuracy of model C is the equal or superior to that of model D above the 94th percentile, whereas model D consistently performs best up to the 94th percentile. In summary, model C is better than model D in terms of predicting extremely high values, and model B yielded the largest prediction error across all percentiles.

6. Discussion and conclusions

We examined the spatial and temporal distribution of mosquito surveillance data collected from Ontario, Canada, between 2005 and 2008. Our primary focus was on *Culex pipiens*, which is known for their preference of urban settings for their habitats. Statistical analyses and mapping revealed strong and statistically significant associations with weather conditions and environmental factors. They included the average temperature, accumulated rainfalls 5 weeks prior to the data collection, elevation, and land-use type such as built-up areas and vegetation areas. We identified the presence of the temporal correlation in mosquito surveillance data and incorporated this in the statistical model.

The warmest spring and summer in 2008 and the coldest summer accompanied with large rainfall in 2007 attributed to the unusually high and low mosquito abundance of each year. Apparently this hotter and longer summer in 2008 contributed to the elongated breeding season of *Culex pipiens* and, consequently, resulted in the high mosquito abundance. It has also been noted that temperature and photoperiod can have an effect on *Culex pipiens* host seeking and induction of diapause behavior (Eldridge 1968; Sanburg and Larsen 1973; Madder et al. 1983). These higher temperatures experienced in 2008 may account for an elongated season. Harmonic analysis facilitated the identification of a coherent seasonal variability of weather conditions and weekly mosquito abundance as evidenced in the correlation analysis; the harmonic predictions of temperature and precipitation have stronger correlations (0.71 and 0.43) with the mean pooled mosquito abundance per trap night than original weather variables (0.61 and 0.41). By decomposing the time series data into different harmonics, we were able to characterize the variability in each variable over the year and detected similarities in amplitude between mosquito abundance and temperature. We also identified the timing of the peak in female adult mosquito adults in relation to temperature and precipitation from the phase values. Visual comparisons of harmonic predictions particularly improved our understanding of the adult mosquito population dynamics with respect to weather conditions in various weather conditions as shown in 2007 and 2008. Our findings are consistent with previous research (Trawinski and MacKay 2008; Soverow et al. 2009; Ruiz et al. 2010) that weekly variation in the mosquito abundance is strongly and positively correlated with coincident and antecedent measure of local climate.

We compared the spatial distribution of mosquito abundance in relation to the spatial intensity of trapping efforts each year. The influence of mosquito surveillance intensity on the spatial patterns of mosquito abundance was visually and statistically investigated using the KDE method and correlation analysis. The results suggested that mosquito abundance was not necessarily induced from intense surveillance efforts. Except the year 2005 when high mosquito surveillance efforts were concentrated on the city of Toronto, the relationship was not found in the other 3 years. We also found that high mosquito abundance areas shifted from the city of Toronto to other neighboring regions, including the border region of Peel and the region of Hamilton, in the following years. Further spatial analysis with detailed environmental data is needed.

To assess the effects of weather and landscape conditions on mosquito abundance under the consideration of the nested structure of data, we proposed mixed effects models with correlated structure. The consideration of random effects for trap sites or trap nights improved the model fit, but it did not substantially affect fixed effects estimates. Empirical variogram analysis for the random effects (models B and C) revealed the presence of strong temporal correlation in model C.

The improved model fit result (the smallest AIC) of model D allowed us to draw a conclusion that a site-specific random effects model with temporal autocorrelation may be the optimal framework for the WNV mosquito surveillance data–driven mosquito abundance model. The landscape variables that established statistically significant associations across all four models include elevation and land-use patterns surrounding trap sites, such as vegetation areas and built-up areas. The negative correlation with elevation might be due to the habitat availability of *Culex pipiens* at higher elevation—the relative scarcity of catch basins due to the better drainage in high elevation. NDVI was not a strong predictor of mosquito abundance unlike other studies (Diuk-Wasser et al. 2006; Bisanzio et al. 2011), although we found the affinity of *Culex pipiens* to urban structures characterized by an urban indicator variable and their preference to built-up areas as well as green areas for their habitats.

Our findings have multiple implications for better understanding of WNV mosquito abundance and potential risk model development in the study region. First, we found a high correlation with weather variables, which provides the opportunity to forecast *Culex pipiens* abundance in the study region and a capability to guide intervention efforts at local and state levels. However, our results are based on the assumption that weather conditions are homogeneous and uniform across study areas, and the generalization of our findings would fail to capture dynamic interactions between the *Culex pipiens* life cycle and environmental variability over time. Chuang et al. (2012) demonstrated the usefulness of the satellite remote sensing data–derived environmental metrics as spatiotemporal predictors of mosquito abundance, although the availability and completeness of the data depends on sparse networks and resource availability. On the other hand, the harmonic analysis used in this paper could be a promising means of characterizing seasonal variability and establishing associations if such remotely sensed data are available for multiple time instants. In addition, we demonstrated that intense trapping efforts have not always been placed at the areas with high mosquito abundance through the retrospective analysis of two spatial density maps—mosquito abundance and trapping efforts. Future mosquito abundance is hard to predict based only on past mosquito surveillance data, but focused analyses on the areas with high mosquito abundance might guide optimal surveillance design in epidemiological studies, which are typically costly and labor intensive. Last, we demonstrated that the proposed site-specific random effects model with temporal autocorrelation addressed the nature of mosquito surveillance data and thus have the potential to improve our understanding of dynamic changes in the mosquito population.

Acknowledgments. The authors thank to the Ontario Agency for Health Protection and Promotion for sharing mosquito surveillance data. This work was supported by a discovery grant from Canada National Science and Engineering Research Council.

References

Anderson, J. F., T. G. Andreadis, A. J. Main, F. J. Ferrandino, and C. R. Vossbrinck, 2006: West Nile virus from female and male mosquitoes (Diptera: Culicidae) in subterranean, ground, and canopy habitats in Connecticut. *J. Med. Entomol.*, **43**, 1010–1019, doi:10.1093/jmedent/43.5.1010.

Anderson, T. K., 2009: Kernel density estimation and k-means clustering to profile road accident hotspots. *Accid. Anal. Prev.*, **41**, 359–364, doi:10.1016/j.aap.2008.12.014.

Bisanzio, D., M. Giacobini, L. Bertolotti, A. Mosca, L. Balbo, U. Kitron, and G. M. Vazquez-Prokopec, 2011: Spatio-temporal patterns of distribution of West Nile virus vectors in eastern piedmont region, Italy. *Parasites Vectors*, **4**, 230, doi:10.1186/1756-3305-4-230.

Bolling, B. G., C. M. Barker, C. G. Moore, W. J. Pape, and L. Eisen, 2009: Seasonal patterns for entomological measures of risk for exposure to *Culex* vectors and West Nile virus in relation to human disease cases in northeastern Colorado. *J. Med. Entomol.*, **46**, 1519–1531, doi:10.1603/033.046.0641.

Briggs, W. L., and V. E. Henson, 1995: *The DFT: An Owners' Manual for the Discrete Fourier Transform.* SIAM, 434 pp.

Brown, H., M. Diuk-Wasser, T. Andreadis, and D. Fish, 2008: Remotely-sensed vegetation indices identify mosquito clusters of West Nile virus vectors in an urban landscape in the northeastern United States. *Vector-Borne Zoonotic Dis.*, **8**, 197–206, doi:10.1089/vbz.2007.0154.

Brownstein, J. S., H. Rosen, D. Purdy, J. R. Miller, M. Merlino, F. Mostashari, and D. Fish, 2002: Spatial analysis of West Nile virus: Rapid risk assessment of an introduced vector-borne zoonosis. *Vector-Borne Zoonotic Dis.*, **2**, 157–164, doi:10.1089/15303660260613729.

Chuang, T.-W., M. B. Hildreth, D. L. Vanroekel, and M. C. Wimberly, 2011: Weather and land cover influences on mosquito populations in Sioux Falls, South Dakota. *J. Med. Entomol.*, **48**, 669–679, doi:10.1603/ME10246.

——, G. M. Henebry, J. S. Kimball, D. L. VanRoekel-Patton, M. B. Hildreth, and M. C. Wimberly, 2012: Satellite microwave remote sensing for environmental modeling of mosquito population dynamics. *Remote Sens. Environ.*, **125**, 147–156, doi:10.1016/j.rse.2012.07.018.

Ciota, A. T., C. L. Drummond, M. A. Ruby, J. Drobnack, G. D. Ebel, and L. D. Kramer, 2012: Dispersal of *Culex* mosquitoes (Diptera: Culicidae) from a wastewater treatment facility. *J. Med. Entomol.*, **49**, 35–42, doi:10.1603/ME11077.

Davis, J. C., 2002: *Statistics and Data Analysis in Geology.* 3rd ed. Wiley, 638 pp.

DeGroote, J. P., R. Sugumaran, and M. Ecker, 2014: Landscape, demographic and climatic associations with human West Nile virus occurrence regionally in 2012 in the United States of America. *Geospat. Health*, **9**, 153–168, doi:10.4081/gh.2014.13.

Deichmeister, J. M., and A. Telang, 2011: Abundance of West Nile virus mosquito vectors in relation to climate and landscape variables. *J. Vector Ecol.*, **36**, 75–85, doi:10.1111/j.1948-7134.2011.00143.x.

Diuk-Wasser, M., H. Brown, T. Andreadis, and D. Fish, 2006: Modeling the spatial distribution of mosquito vectors for West Nile virus in Connecticut, USA. *Vector-Borne Zoonotic Dis.*, **6**, 283–295, doi:10.1089/vbz.2006.6.283.

Dohm, D., M. O'Guinn, and M. Turell, 2002: Effect of environmental temperature on the ability of *Culex pipiens* (Diptera: Culicidae) to transmit West Nile virus. *J. Med. Entomol.*, **39**, 221–225, doi:10.1603/0022-2585-39.1.221.

Eldridge, B. F., 1968: The effect of temperature and photoperiod on blood-feeding and ovarian development in mosquitoes of the *Culex pipiens* complex. *Amer. J. Trop. Med. Hyg.*, **17**, 133–140.

Epstein, P. R., 2001: Climate change and emerging infectious diseases. *Microbes Infect.*, **3**, 747–754, doi:10.1016/S1286-4579(01)01429-0.

——, 2005: Climate change and human health. *N. Engl. J. Med.*, **353**, 1433–1436, doi:10.1056/NEJMp058079.

Gardner, A. M., T. K. Anderson, G. L. Hamer, D. E. Johnson, K. E. Varela, E. D. Walker, and M. O. Ruiz, 2013: Terrestrial vegetation and aquatic chemistry influence larval mosquito abundance in catch basins, Chicago, USA. *Parasites Vectors*, **6**, 9, doi:10.1186/1756-3305-6-9.

Gingrich, J. B., R. D. Anderson, G. M. Williams, L. O'Connor, and K. Harkins, 2006: Stormwater ponds, constructed wetlands, and other best management practices as potential breeding sites for West Nile virus vectors in Delaware during 2004. *J. Amer. Mosq. Control Assoc.*, **22**, 282–291, doi:10.2987/8756-971X(2006)22[282:SPCWAO]2.0.CO;2.

Hayes, E. B., N. Komar, R. S. Nasci, S. P. Montgomery, D. R. O'Leary, and G. L. Campbell, 2005: Epidemiology and transmission dynamics of West Nile virus disease. *Emerg. Infect. Dis.*, **11**, 1167–1173, doi:10.3201/eid1108.050289a.

Horsfall, W. R., 1955: *Mosquitoes: Their Bionomics and Relation to Disease*. Ronald Press, 723 pp.

Jakubauskas, M. E., D. R. Legates, and J. H. Kastens, 2001: Harmonic analysis of time-series AVHRR NDVI data. *Photogramm. Eng. Remote Sens.*, **67**, 461–470.

Jones, K., 2004: An introduction to statistical modeling. *Research Methods in the Social Sciences*, C. Lewin and B. Somekh, Eds., Sage, 241–255.

Justino, F., A. Setzer, T. J. Bracegirdle, D. Mendes, A. Grimm, G. Dechiche, and C. Schaefer, 2011: Harmonic analysis of climatological temperature over Antarctica: Present day and greenhouse warming perspectives. *Int. J. Climatol.*, **31**, 514–530, doi:10.1002/joc.2090.

Kilpatrick, A. M., and W. J. Pape, 2013: Predicting human West Nile virus infections with mosquito surveillance data. *Amer. J. Epidemiol.*, **178**, 829–835, doi:10.1093/aje/kwt046.

——, M. A. Meola, R. M. Moudy, and L. D. Kramer, 2008: Temperature, viral genetics, and the transmission of West Nile virus by *Culex pipiens* mosquitoes. *PLoS Pathog.*, **4**, e1000092, doi:10.1371/journal.ppat.1000092.

Komar, N., and G. G. Clark, 2006: West Nile virus activity in Latin America and the Caribbean. *Rev. Panam. Salud Publica*, **19**, 112–117, doi:10.1590/S1020-49892006000200006.

Lebl, K., K. Brugger, and F. Rubel, 2013: Predicting *Culex pipiens/restuans* population dynamics by interval lagged weather data. *Parasites Vectors*, **6**, 129, doi:10.1186/1756-3305-6-129.

Legates, D. R., and C. J. Willmott, 1990: Mean seasonal and spatial variability in global surface air temperature. *Theor. Appl. Climatol.*, **41**, 11–21, doi:10.1007/BF00866198.

Madder, D., G. Surgeoner, and B. Helson, 1983: Induction of diapause in *Culex pipiens* and *Culex restuans* (Diptera: Culicidae) in southern Ontario. *Can. Entomol.*, **115**, 877–883, doi:10.4039/Ent115877-8.

Merritt, R., R. Dadd, and E. Walker, 1992: Feeding behavior, natural food, and nutritional relationships of larval mosquitoes. *Annu. Rev. Entomol.*, **37**, 349–374, doi:10.1146/annurev.en.37.010192.002025.

Moody, A., and D. M. Johnson, 2001: Land-surface phenologies from AVHRR using the discrete Fourier transform. *Remote Sens. Environ.*, **75**, 305–323, doi:10.1016/S0034-4257(00)00175-9.

O'Sullivan, D., and D. Unwin, 2003: *Geographic Information Analysis.* Wiley, 436 pp.

Ozdenerol, E., G. N. Taff, and C. Akkus, 2013: Exploring the spatio-temporal dynamics of reservoir hosts, vectors, and human hosts of West Nile virus: A review of the recent literature. *Int. J. Environ. Res. Public Health*, **10**, 5399–5432, doi:10.3390/ijerph10115399.

Reisen, W., Y. Fang, and V. Martinez, 2006: Effects of temperature on the transmission of West Nile virus by *Culex tarsalis* (Diptera: Culicidae). *J. Med. Entomol.*, **43**, 309–317, doi:10.1093/jmedent/43.2.309.

Rosà, R., and Coauthors, 2014: Early warning of West Nile virus mosquito vector: Climate and land use models successfully explain phenology and abundance of *Culex pipiens* mosquitoes in north-western Italy. *Parasites Vectors*, **7**, 269, doi:10.1186/1756-3305-7-269.

Ruiz, M., and Coauthors, 2010: Local impact of temperature and precipitation on West Nile virus infection in *Culex* species mosquitoes in northeast Illinois, USA. *Parasites Vectors*, **3**, 19, doi:10.1186/1756-3305-3-19.

Sanburg, L. L., and J. R. Larsen, 1973: Effect of photoperiod and temperature on ovarian development in *Culex pipiens pipiens*. *J. Insect Physiol.*, **19**, 1173–1190, doi:10.1016/0022-1910(73)90202-3.

Silverman, B. W., 1986: *Density Estimation for Statistics and Data Analysis.* Vol. 26. CRC Press, 175 pp.

Soverow, J., G. Wellenius, D. Fisman, and M. Mittleman, 2009: Infectious disease in a warming world: How weather influenced West Nile virus in the United States (2001–2005). *Environ. Health Perspect.*, **117**, 1049–1052, doi:10.1289/ehp.0800487.

Trawinski, P. R., and D. MacKay, 2008: Meteorologically conditioned time-series predictions of West Nile virus vector mosquitoes. *Vector-Borne Zoonotic Dis.*, **8**, 505–521, doi:10.1089/vbz.2007.0202.

——, and ——, 2010: Identification of environmental covariates of West Nile virus vector mosquito population abundance. *Vector-Borne Zoonotic Dis.*, **10**, 515–526, doi:10.1089/vbz.2008.0063.

U.S. Environmental Protection Agency, 2004: Wetlands and West Nile Virus. Accessed 19 December 2014. [Available online at http://nepis.epa.gov/Exe/ZyPDF.cgi?Dockey=30005UPA.PDF.]

Wang, J., N. H. Ogden, and H. Zhu, 2011: The impact of weather conditions on *Culex pipiens* and *Culex restuans* (Diptera: Culicidae) abundance: A case study in Peel region. *J. Med. Entomol.*, **48**, 468–475, doi:10.1603/ME10117.

Yoo, E.-H., 2013: Exploring space-time models for West Nile virus mosquito abundance data. *Appl. Geogr.*, **45**, 203–210, doi:10.1016/j.apgeog.2013.09.007.

——, 2014: Site-specific prediction of West Nile virus mosquito abundance in greater Toronto area using generalized linear mixed models. *Int. J. Geogr. Inf. Sci.*, **28**, 296–313, doi:10.1080/13658816.2013.837909.

——, D. Chen, and C. Russel, 2014: West Nile virus mosquito abundance modeling using non-stationary spatiotemporal geostatistics. *Analyzing and Modeling Spatial and Temporal Dynamics of Infectious Diseases*, D. Chen, B. Moulin, and J. Wu, Eds., John Wiley and Sons, 263–282.

Zuur, A., E. Leno, N. Walker, A. Saveliev, and G. Smith, 2009: *Mixed Effects Models and Extensions in Ecology with R.* Springer, 574 pp.